Time-Resolved EPR Study of Electron–Hole Dissociations Influenced by Alkyl Side Chains at the Photovoltaic Polyalkylthiophene:PCBM Interface

ARTICLE *in* JOURNAL OF PHYSICAL CHEMISTRY LETTERS · DECEMBER 2013

Impact Factor: 7.46 · DOI: 10.1021/jz402300m

3 AUTHORS, INCLUDING:

Yasuhiro Kobori
Kobe University
48 PUBLICATIONS **837** CITATIONS

SEE PROFILE

THE JOURNAL OF PHYSICAL CHEMISTRY Letters

Letter

pubs.acs.org/JPCL

Time-Resolved EPR Study of Electron−Hole Dissociations Influenced by Alkyl Side Chains at the Photovoltaic Polyalkylthiophene:PCBM Interface

Taku Miura,[†] Motoko Aikawa,[†] and Yasuhiro Kobori*[,‡,§]

[†]Department of Chemistry, Graduate School of Science, Shizuoka University, 836 Ohya Suruga-ku, Shizoka 422-8529, Japan

[‡]Department of Chemistry, Graduate School of Science, Kobe University, 1-1 Rokkoudai-cho, Nada-ku, Kobe 657-8501, Japan

[§]PRESTO, Japan Science and Technology Agency, 4-1-8 Honcho Kawaguchi-shi, Saitama 332-0012, Japan

Supporting Information

ABSTRACT: Nanosecond time-resolved electron paramagnetic resonance (TREPR) spectroscopy has been utilized at T = 77 K to characterize alkyl side-chain effects on geometries and on the electronic couplings (V_{CR}) of transient charge-separated (CS) states in the photoactive layers fabricated by the spin-coating of mixed solutions of regioregular polyalkylthiophenes (RR-P3AT) and [6,6]-C_{61}-butyric acid methyl ester (PCBM). By increasing the alkyl side-chain number from 6 to 12 in P3AT, a highly distant and long-lived CS state has been obtained. This result is explained by a coupling of the hole dissociation to the polymer librations by the side-chains. From an exponential decay of V_{CR} with respect to the CS distance, the attenuation factor (β_e) has been determined to be β_e = 0.2 Å^{-1}. Such a long-range tunneling feature is explained by the generations of the shallowly trapped, delocalized electron−hole pairs by the dissociation of the hole toward π-stacking directions at the organic photovoltaic interface.

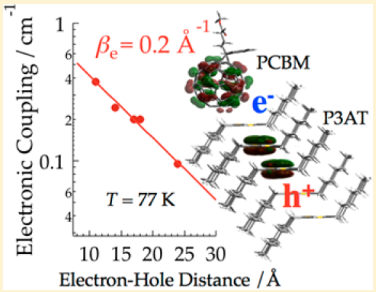

SECTION: Energy Conversion and Storage; Energy and Charge Transport

Organic bulkheterojunction (BHJ) thin-films composed of the conjugated polymers as the electron donors (D) and [6,6]-C_{61}-butyric acid methyl ester (PCBM) as the electron acceptor (A) have been regarded as one of the attractive materials for low cost and flexible solar-cell devices.[1,2] In the photoactive layer of the BHJ film, the polymer-fullerene phase segregation is in the range of 5−10 nm, which is the excition diffusion length.[3] This small domain size contributes to the efficient photoinduced charge-transfer (CT) reaction at the polymer-fullerene interface. One of the puzzling subjects has been that most of the electrons and holes generated at the interface escape from the CT binding by the Coulomb attraction whose energy is supposed to be several hundreds of millielectron-volts for the low dielectric environment ($\varepsilon_r \approx 3$) in the solid blends.[4−7] Baranovskii et al.[8] have recently proposed that the strong Coulomb attraction is reduced by the interfacial discrete dipole arrays distributed in the dark at the D−A domain interface.[9]

The molecular motion in the organic semiconductors is another key to the efficient carrier dissociation. The molecular libration in the blend should enhance the entropy of the dissociated CS state as compared to that of the bound CT state as emphasized by Clarke and Durrant.[7] Following pioneering time-resolved electron paramagnetic resonance (TREPR) works[10,11] on related blend materials, we have measured and analyzed the TREPR spectra of the blends by poly(3-hexylthiophene-2,5-diyl) (P3HT) and PCBM at 77 K[12] to characterize the nanostructure, the electronic coupling (V_{CR}), and the motion of the spin correlated radical pair (SCRP)[13,14] of P3HT$^{+\bullet}$−PCBM$^{-\bullet}$. Numerous studies have been performed to clarify the carrier dissociation mechanism in the organic semiconductors.[3−5,7,8,11,12,15−17] However, only a few studies have experimentally elucidated the effects of the polymer motions on the carrier dissociation. Moreover, despite the importance of the electronic character of the distant CS systems,[18−21] no study has determined the distance dependence of the V_{CR} for understanding the nature of the electron tunneling to contribute to the charge transport at the BHJ domain interface. In the present Letter, by using the TREPR spectroscopy, we have examined effects of the alkyl side-chains on the electron−hole dissociation and on the V_{CR} of the transient CS state for the regioregular polyalkylthiophene (RR-P3AT):PCBM blend films fabricated by the spin coating method.

Geometries and Exchange Couplings of the Photoinduced CS States. Figure 1 shows examples of the TREPR data obtained by nanosecond 532 nm laser irradiations at T = 77 K of spin-coated thin films (spun at 3000 rpm for 30 s on a glass substrate as detailed in the Supporting Information). At the left, TREPR spectra are shown for the film fabricated from the RR-P3HT:PCBM (1:1 by weight) dissolved in 1,2-dichlorobenzene. The right spectra are from the 1:1 blend of regioregular

Received: October 24, 2013
Accepted: December 3, 2013
Published: December 24, 2013

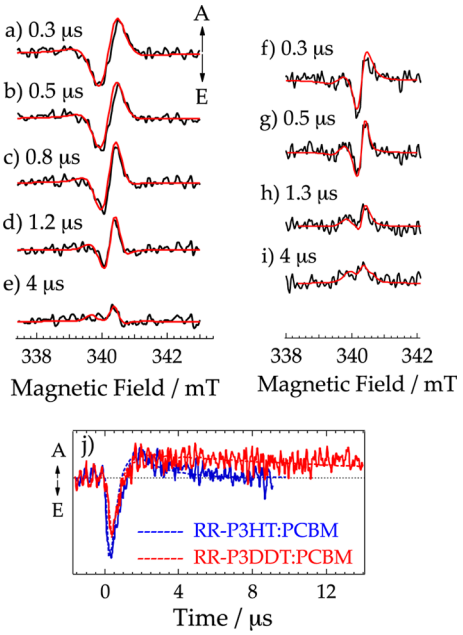

Figure 1. (a–e): TREPR spectra of the thermally annealed film of the RR-P3HT:PCBM blend obtained at several delay times after the 532 nm laser excitations at T = 77 K. (f–i): TREPR spectra of the as-spun film of the RR-P3DDT:PCBM blend at T = 77 K. (j) Time evolutions in the transient EPR of the initial emissive signals for the as-spun RR-P3HT:PCBM (blue line) and for the as-spun RR-P3DDT:PCBM (red line). The red spectra and the dashed lines in the time traces are simulated by the SLE calculations.

poly(3-dodecylthiophene-2,5-diyl) (RR-P3DDT):PCBM. The positive signal denoted by 'A' is the microwave absorption, while the negative direction of 'E' is the emission. The signal field positions in Figure 1 were consistent with the resonance positions of the dissociated polarons of $P3AT^{+\cdot}$ and $PCBM^{-\cdot}$ obtained by steady-state EPR measurements[12,22] (not shown) using standard phase-sensitive detections. The initial A/E/A/E pattern (Figure 1a and Figure S2) and the E/A/E/A (Figure 1f) are attributed to the SCRP signal affected by the spin-dipolar interaction (D) between $P3AT^{+\bullet}$ and $PCBM^{-\bullet}$ in the transient CS states.[12] At 1.2 μs, both in Figure 1d and 1h, the net absorptive polarization is imposed and is explained by the thermal equilibrium population generated by the spin–lattice relaxation in the SCRP. Figure 1j shows time profiles of the TREPR of the initial emissive signals for the as-spun RR-P3HT:PCBM film (as reported in Figure S3) and for the RR-P3DDT:PCBM film. The initial emissive signals are quickly deactivated within ca. 1 μs and are attributed to the spin–lattice relaxation[12] in the SCRP. The decay of the absorption in the blue line is attributed to the deactivation of the triplet CS character to generate the triplet excition in the P3AT moiety.[12]

As shown in the TREPR spectra in Figure 1f–i, by replacing the hexyl side chains with the dodecyl ones in the polyalkylthiophen, the spectrum widths become much smaller compared with the widths in Figure 1a–e, denoting that the spin dipolar interaction is significantly weakened in the CS state. Evidently, the decay of the thermal equilibrium absorption (red line) in Figure 1j is much slower in the P3DDT:PCBM system than in the P3HT:PCBM system (blue line), indicating that the charge-recombination (CR) is highly suppressed. These results are explained by the initial generation of the highly distant CS state by the electron–hole dissociation in the P3DDT:PCBM.

To clarify the electron–hole dissociation mechanism and the electronic property in the photoinduced CS states, the nanostructures and the singlet–triplet ($S-T_0$) energy gaps (exchange coupling: $2J$) are determined from the simulation of the TREPR data (the red lines in the TREPR spectra and the dashed lines in the time traces in Figure 1). These simulations are based on the stochastic-Liouville equation (SLE) by which the time-dependent quantum mechanical phenomena in the density matrix ($\boldsymbol{\rho}$) of the singlet–triplet system are solved[12] in the rotating frame on the basis spin-functions of $|+\rangle = |\alpha\alpha\rangle$, $|0\rangle = |\alpha\beta + \beta\alpha\rangle/\sqrt{2}$, $|-\rangle = |\beta\beta\rangle$ for the triplet CS state, and of $|S\rangle = |\alpha\beta - \beta\alpha\rangle/\sqrt{2}$ for the singlet CS state. As detailed in the Supporting Information (SI), the effects of the spin relaxations (the spin–lattice relaxation time of T_1, the transverse relaxation time T_2 and the relaxation time of T_{23} by the $S-T_0$ dephasing) and the charge-recombination (CR) kinetics are taken into account in the analysis. The spin Hamiltonian H_0 of the radical pair is composed of the Zeeman interaction, the hyperfine interactions, the spin–spin exchange coupling (J), and the spin-dipolar coupling (D) as reported previously.[12] The Euler angles of the principal g-axis system of $PCBM^{-\bullet}$ with respect to the g-

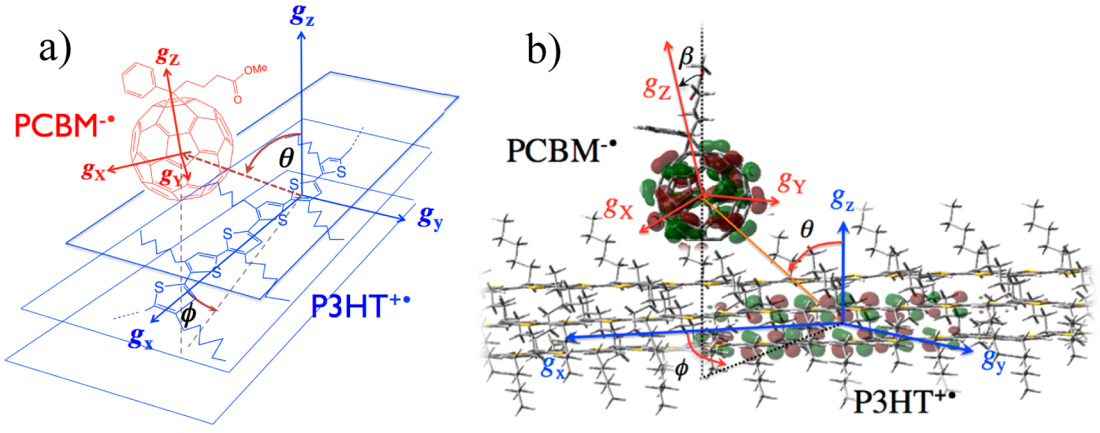

Figure 2. Schematic views of the interfacial CS geometry to reproduce the TREPR spectra (left in Figure 1) for the thermally annealed film of the RR-P3HT:PCBM blend. $PCBM^{-\bullet}$ is located on the top of the aromatic planes (shown by the rectangles at the left) by the π-stacked RR-P3HT chains at the crystalline region in panels a and b, while the spin density in $P3AT^{+\bullet}$ is delocalized around the second and third aromatic layers as shown in b.

dx.doi.org/10.1021/jz402300m | J. Phys. Chem. Lett. 2014, 5, 30–35

Table 1. Parameters for the Simulations (Red and Blue Lines in Figure 1) of the Time-Dependent EPR Spectra of the Photoinduced CS States in the RR-P3AT:PCBM Blend Films

blend films	D/mT	J/μT	$k_{CRT}/10^5$ s^{-1a}	T_1/μs^b	dipolar angles^c	Euler angles^d	$\lvert V_{CR}\rvert$/cm^{-1}
RR-P3HT:PCBM (as-spun)	−0.63	12	10	0.5	θ = 50° ϕ = 35°	α = 51° β = 18° γ: arbitrary	0.25
RR-P3HT:PCBM (thermally annealed)	−0.46	8.2	4.0	1.0	θ = 44° ϕ = 34°	α = −50° β = 18° γ: arbitrary	0.20
RR-P3DDT:PCBM (as-spun)	−0.20	1.8	0.83	0.5	θ = 45° ϕ = 60°	α = 10° β = 15° γ: arbitrary	0.09

[a]Charge-recombination rate constant from the triplet CS state. [b]Spin−lattice relaxation time. [c]Direction of the dipolar principal axis between $P3AT^{+\bullet}$ and $PCBM^{-\bullet}$ defined by the polar angles with respect to the principal g-tensor axes in $P3AT^{+\bullet}$ as shown in Figure 2. [d]Euler angles of the principal g-axis system of $PCBM^{-\bullet}$ with respect to the g-axis system in $P3AT^{+\bullet}$.

axis system in $P3AT^{+\bullet}$ are defined by (α, β, γ) with the x-convention. Details of the principal g-values[22] in Figure 2 are reported in our previous study.[12] The spin relaxation parameters are detailed in the SI. Table 1 summarizes the parameters to reproduce the TREPR data in Figure 1. Fitting errors are less than ±0.5 μT for the exchange couplings and are ±2° for the angle parameters.

From Table 1 and the anticipated hole delocalization character in $P3AT^{+\bullet}$ by the dimer polaron model[23] in the P3AT crystalline domain, one of the nanostructures of the CS states is depicted for the thermally annealed RR-P3HT:PCBM film in Figure 2. The structure of $P3AT^{+\bullet}$ in the P3AT region is based upon a recent electron diffraction analysis that has revealed a tilted packing structure with the short $\pi-\pi$ stacking of a 3.4 Å interplanar distance in the crystalline P3HT.[24,25] It should, however, be noted that because of the fast spin relaxation times ($T_1 < \sim 1$ μs and T_2 of 10−50 ns as reported in the SI) even at T = 77 K, the positions and orientations of the unpaired spins are distributed or fluctuated around the structure in Figure 2.[12] For the as-spun RR-P3HT:PCBM, a fast S−T_0 dephasing time (T_{23} = 1.2 μs) is required to completely reproduce the delay time dependence of the TREPR spectra (Figure S3a−e). Since the S−T_0 dephasing is induced by the fluctuations of the exchange and the dipolar couplings,[26] the libration motions in the unpaired spins are conclusive. After the treatment of the thermal annealing in Table 1, the dipolar coupling becomes weaker from −0.63 mT to −0.46 mT. Since the charge mobility of $PCBM^{-\bullet}$ is much smaller at 77 K than the mobility of $P3HT^{+\bullet}$ in the RR-P3HT:PCBM blend,[27] the weaker dipolar coupling denotes that the hole is more separated at the domain interface by the annealing treatment. From Table 1, the angle of θ is decreased from 50° to 44° by the annealing. Connecting the separated hole with the decrease in θ, it is concluded that $P3HT^{+\bullet}$ has been separated not to the intrachain direction in the conjugated polymer (horizontal direction in Figure 2) but to the interchain direction (lower direction in Figure 2). In the RR-P3DDT:PCBM system, the dipolar coupling becomes much weaker (−0.20 mT), while θ is decreased from 50° to 45° for the as-spun films. These results also denote that the interchain hole dissociation is taking place toward the π-stacking direction at the RR-P3DDT:PCBM interface. Figure 3 summarizes the side views of the transient interfacial electron−hole pairs from the simulation of the TREPR spectra. In Figure 3a, we assume that the delocalized hole in P3HT is distributed at the surface

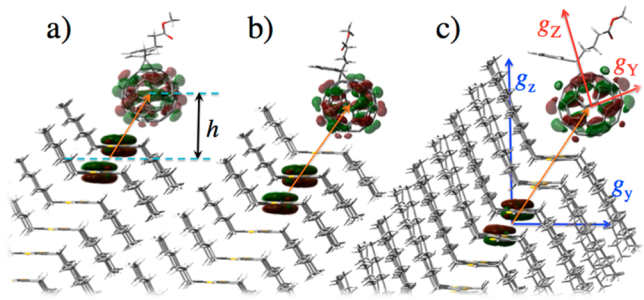

Figure 3. Views from the long polymer axis (g_x axis in Figure 2a) of the geometries of the interfacial photoinduced CS states in (a) the as-spun RR-P3HT:PCBM film (r_{CC} = 14 Å), (b) the annealed RR-P3HT:PCBM film (r_{CC} = 17 Å), and (c) the as-spun RR-P3DDT:PCBM film (r_{CC} = 24 Å).

layer of the interface for the as-spun film as has been reported on the cast P3HT:PCBM films in the previous study.[12]

In Figure 3a, the height (h) is obtained to be h = 8.8 Å from the g_x-g_y plane to the center position of the C_{60} sphere by summing the 1.7 Å height (= half of the 3.4 Å interplanner stacking distance in P3HT) and the reported edge-to-edge stacking distance (3.5 Å)[28] between the P3HT and the PCBM molecules, and the radius (3.6 Å) of the C_{60} sphere. From θ = 50°, the center-to-center distance (r_{CC}) between the unpaired orbitals is obtained to be $r_{CC} = h/\cos\theta$ = 14 Å for the orange straight line in Figure 3a.[12] From the simple point-dipole approximation,[29] r_{CC} = 16 Å gives the spin dipolar coupling of D = −0.63 mT in Table 1. Considering the interchain delocalized hole distribution in Figure 3a to weaken the dipolar interaction, r_{CC} = 14 Å is a reasonable center separation to provide D = −0.63 mT in Figure 3a. By the same procedure as in Figure 3a, r_{CC} = 17 Å is obtained for the thermally annealed film in Figure 3b and is reasonably close to 18 Å calculated from the point-dipole approximation to give D = −0.46 mT in Table 1. In the RR-P3DDT:PCBM system, the highly dissociated electron−hole pair has been obtained in Figure 3c, thus r_{CC} = 24 Å is determined using the point-dipole approximation to provide D = −0.20 mT in Figure 3c.

Hole Dissociation Mechanism at the Organic Photovoltaic Interfaces. From Figure 3c, it is evident that the dodecyl side-chains in P3AT induce the more separated electron−hole pairs. Recent studies have demonstrated that the photoinduced, contact charge-transfer (CT) states are initially generated at the D/A domain-interfaces in the P3AT:PCBM,[4] indicating that the fast distant hole dissociations occur from the bound CT

dx.doi.org/10.1021/jz402300m | J. Phys. Chem. Lett. 2014, 5, 30−35

states to provide the highly separated CS states. Thus, the hole dissociations are explained by an effect of a coupling of the hole to the librations (phonon)[30] of the P3AT crystalline domains; the increase in the side-chain's number promotes the motions of the alkyl side-chains due to the significant increase in the vibration modes that couple to the unpaired orbital in Figure 3. Such electron−phonon (e−p) coupling contributes to the instantaneous interchain mobility for the hole dissociations.[30] It is also considered that the increase in the vibration modes enhances the entropy for the hole dissociations, stabilizing the more distant CS states. The thermal annealing effect on the hole dissociation from Figure 3a to 3b is similarly explained by the side-chain motions in P3AT, as follows. Recent X-ray diffraction analyses of the RR-P3HT:PCBM blend films reported that the P3HT domain size is increased by thermal annealing due to a permanent lamellar stretching just along the alkyl-stacking direction.[24] This lamellar stretching can induce the disordered conformations of the end group ($-CH_3$) in the hexyl chain because of the lack of the rotational restrictions in $-CH_3$ by the alkyl-stacking interactions.[31] Such disordered motions by the side-chains can enhance both the e−p coupling and the entropy for the hole dissociations to stabilize the more separated electron−hole pairs in Figure 3b than in the as-spun RR-P3HT:PCBM.

Electronic Tunneling Barrier of the Distant Electron−Hole Pairs. From the $2J$ parameters in Table 1, one can estimate the $|V_{CR}|$ values for the CR to the excited triplet P3AT using the relationship of the configuration interaction;[21,32,33] $2J = |V_{CR}|^2/\Delta E_{CR}$, where ΔE_{CR} (~0.4 eV)[12] is the vertical energy gap for the triplet CR. In Table 1, the determined $|V_{CR}|$ values are listed for the CS states. It has been found in Table 1 that $|V_{CR}|^2$ values are correlated with the k_{CRT} values determined by the decays of the absorptive signals in Figure 1. This result strongly supports the validity of the $|V_{CR}|$ determinations since k_{CRT} is proportional to $|V_{CR}|^2$ according to Marcus theory as detailed in the SI.[34] The $|V_{CR}|$ values in Table 1 have been plotted with respect to the r_{CC} values, together with the $|V_{CR}|$ reported for the cast films of the regiorandom-P3HT:PCBM ($|V_{CR}|$ = 0.4 cm^{-1} for r_{CC} = 11 Å, which is estimated by $D = -2.1$ mT) and of the RR-P3HT:PCBM blend ($|V_{CR}|$ = 0.2 cm^{-1} for r_{CC} = 18 Å) in the previous study.[12]

From the semilog plot in Figure 4, it is evident that the electronic coupling decays by a single exponential function as r_{CC} is increased. Such decays have been characterized by the attenuation factor of β_e in $|V_{CR}| = V_0 \exp(-\beta_e (r_{CC} - r_0)/2)$ as shown by the red line in Figure 4.[18,35] The least-squares fitting (red line) of the plots yields β_e = 0.2 $Å^{-1}$. In the DNA hairpin systems that generate the photoinduced CS states of $G^{+\bullet}-(T)_m-S^{-\bullet}$ in which T and G represent the stacking thymine and guanine bases, respectively,[36] β_e = 0.9 $Å^{-1}$ has been obtained for the CR processes. The features of β_e < 2 $Å^{-1}$ have been explained by the superexchange electron-tunneling model mediated by the intervening electronic states between the unpaired orbitals.[18,21] Using the McConnell's tunneling model,[37] β_e can been approximated as follows:[35,38]

$$\beta_e = \frac{2}{d_{BB}} \ln\left(\frac{\Delta E_{eff}}{V_{BB}}\right) \quad (1)$$

where d_{BB} and V_{BB} are the bridge-to-bridge stacking distance and the transfer integral between the bridging chromophores, respectively. ΔE_{eff} is the vertical energy gap for the holes to oxidize the bridge units. From the oxidation potential difference between T and G, ΔE_{eff} = 0.7 eV is evaluated in the DNA hairpins.[36] d_{BB} = 3.4 Å and V_{BB} = 0.16 eV are estimated for the π-stacking distances and for the π-stacking interactions, respectively both in the DNAs[39] and in the crystalline domains of P3AT[40] in Figure 3. To fit β_e = 0.2 $Å^{-1}$ using eq 1, ΔE_{eff} = 0.2 eV is obtained as the tunneling barrier from the delocalized holes in the P3AT region of Figure 2 to the highest occupied molecular orbitals (HOMO) of the single P3AT chains. This energy gap is comparable to V_{BB} and is consistent with the dimer polaron model[23] that explains the shift of the optical absorption band of the delocalized polarons by the π-stacking in the P3HT region. Equation 1 is based upon the perturbation theory under the assumption of $\Delta E_{eff} \gg V_{BB}$. Thus, the evaluated ΔE_{eff} would include an uncertainty since $\Delta E_{eff} \approx V_{BB}$ is obtained. However, the small tunneling barrier with $\Delta E_{eff} \approx V_{BB}$ implies that the transient holes in Figure 3 are energetically located at a level very close to the valence band in the P3AT crystalline domain, since additional stabilization or reorganization energies are required by the lattice defects for the deeper trap sites of the polarons, that is, $\Delta E_{eff} \gg V_{BB}$ for the deeply trapped CS states.

In conclusion, by using TREPR, the quite long-range electronic coupling with β_e = 0.2 $Å^{-1}$ has been characterized for the transient CS states at the domain interfaces. Such a molecular wire property is explained by the shallow traps of the unpaired orbitals in the P3AT domains, while the larger β_e (= 0.9 $Å^{-1}$) has been explained by the deeper trap by $G^{+\bullet}$ with respect to T in the $G^{+\bullet}$-$(T)_m$-$S^{-\bullet}$ of the DNA hairpins. This unique molecular-wire behavior and the effect of the side-chain motions on the carrier dissociations in the present organic photovoltaic interface should be keys for the designs and characterizations of more efficient organic active layers.

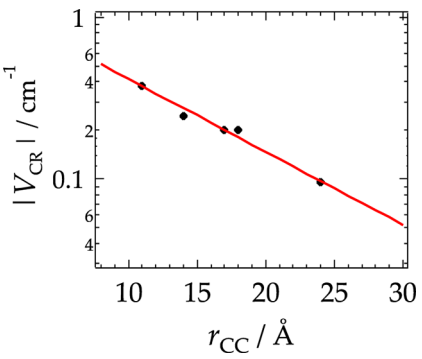

Figure 4. Semilog plot of $|V_{CR}|$ versus r_{CC} of the electron−hole pairs in Figure 3 in the several P3AT:PCBM (1:1) blend materials prepared from the 1,2-dichlorobenzene solutions. β_e = 0.2 $Å^{-1}$ is obtained as the attenuation factor in the exponential decay of the electronic coupling.

■ ASSOCIATED CONTENT

Supporting Information

Details of the sample preparations, the experimental methods, the theoretical treatments of the spin relaxation parameters using the SLE, and the validity of the attenuation factor considered by the superexchange model. This material is available free of charge via the Internet at http://pubs.acs.org.

■ AUTHOR INFORMATION

Corresponding Author

*E-mail: ykobori@kitty.kobe-u.ac.jp.

Notes

The authors declare no competing financial interest.

■ ACKNOWLEDGMENTS

The authors thank Prof. Hisao Murai (Shizuoka University) for experimental support and useful discussions. This work was supported by a Grant-in-Aid for Scientific Research (No. 25288004) from the Ministry of Education, Culture, Sports, Science and Technology, Japan.

■ REFERENCES

(1) Yu, G.; Gao, J.; Hummelen, J. C.; Wudl, F.; Heeger, A. J. Polymer Photovoltaic Cells: Enhanced Efficiencies via a Network of Internal Donor−Acceptor Heterojunctions. *Science* **1995**, *270*, 1789−1791.

(2) Kim, Y.; Cook, S.; Tuladhar, S. M.; Choulis, S. A.; Nelson, J.; Durrant, J. R.; Bradley, D. D. C.; Giles, M.; Mcculloch, I.; Ha, C. S.; Ree, M. A Strong Regioregularity Effect in Self-Organizing Conjugated Polymer Films and High-Efficiency Polythiophene:Fullerene Solar Cells. *Nat. Mater.* **2006**, *5*, 197−203.

(3) Guo, J. M.; Ohkita, H.; Benten, H.; Ito, S. Charge Generation and Recombination Dynamics in Poly(3-hexylthiophene)/Fullerene Blend Films with Different Regioregularities and Morphologies. *J. Am. Chem. Soc.* **2010**, *132*, 6154−6164.

(4) Lee, J.; Vandewal, K.; Yost, S. R.; Bahlke, M. E.; Goris, L.; Baldo, M. A.; Manca, J. V.; Van Voorhis, T. Charge Transfer State Versus Hot Exciton Dissociation in Polymer-Fullerene Blended Solar Cells. *J. Am. Chem. Soc.* **2010**, *132*, 11878−11880.

(5) Bakulin, A. A.; Rao, A.; Pavelyev, V. G.; van Loosdrecht, P. H. M.; Pshenichnikov, M. S.; Niedzialek, D.; Cornil, J.; Beljonne, D.; Friend, R. H. The Role of Driving Energy and Delocalized States for Charge Separation in Organic Semiconductors. *Science* **2012**, *335*, 1340−1344.

(6) Murthy, D. H. K.; Gao, M.; Vermeulen, M. J. W.; Siebbeles, L. D. A.; Savenije, T. J. Mechanism of Mobile Charge Carrier Generation in Blends of Conjugated Polymers and Fullerenes: Significance of Charge Delocalization and Excess Free Energy. *J. Phys. Chem. C* **2012**, *116*, 9214−9220.

(7) Clarke, T. M.; Durrant, J. R. Charge Photogeneration in Organic Solar Cells. *Chem. Rev.* **2010**, *110*, 6736−6767.

(8) Baranovskii, S. D.; Wiemer, M.; Nenashev, A. V.; Jansson, F.; Gebhardt, F. Calculating the Efficiency of Exciton Dissociation at the Interface between a Conjugated Polymer and an Electron Acceptor. *J. Phys. Chem. Lett.* **2012**, *3*, 1214−1221.

(9) Marchiori, C. F. N.; Koehler, M. Dipole Assisted Exciton Dissociation at Conjugated Polymer/Fullerene Photovoltaic Interfaces: A Molecular Study Using Density Functional Theory Calculations. *Synth. Met.* **2010**, *160*, 643−650.

(10) Franco, L.; Ruzzi, M.; Corvaja, C. Time-Resolved Electron Paramagnetic Resonance of Photoinduced Ion Pairs in Blends of Polythiophene and Fullerene Derivatives. *J. Phys. Chem. B* **2005**, *109*, 13431−13435.

(11) Behrends, J.; Sperlich, A.; Schnegg, A.; Biskup, T.; Teutloff, C.; Lips, K.; Dyakonov, V.; Bittl, R. Direct Detection of Photoinduced Charge Transfer Complexes in Polymer Fullerene Blends. *Phys. Rev. B* **2012**, *85*, 125206.

(12) Kobori, Y.; Noji, R.; Tsuganezawa, S. Initial Molecular Photocurrent: Nanostructure and Motion of Weakly Bound Charge-Separated State in Organic Photovoltaic Interface. *J. Phys. Chem. C* **2013**, *117*, 1589−1599.

(13) Hore, P. J.; Hunter, D. A.; McKie, C. D.; Hoff, A. J. Electron Paramagnetic Resonance of Spin-Correlated Radical Pairs in Photosynthetic Reactions. *Chem. Phys. Lett.* **1987**, *137*, 495−500.

(14) Closs, G. L.; Forbes, M. D. E.; Norris, J. R. Spin-Polarized Electron-Paramagnetic Resonance-Spectra of Radical Pairs in Micelles - Observation of Electron Spin−Spin Interactions. *J. Phys. Chem.* **1987**, *91*, 3592−3599.

(15) Isaacs, E. B.; Sharifzadeh, S.; Ma, B. W.; Neaton, J. B. Relating Trends in First-Principles Electronic Structure and Open-Circuit Voltage in Organic Photovoltaics. *J. Phys. Chem. Lett.* **2011**, *2*, 2531−2537.

(16) D'avino, G.; Mothy, S.; Muccioli, L.; Zannoni, C.; Wang, L. J.; Cornil, J.; Beljonne, D.; Castet, F. Energetics of Electron-Hole Separation at P3HT/PCBM Heterojunctions. *J. Phys. Chem. C* **2013**, *117*, 12981−12990.

(17) Niklas, J.; Mardis, K. L.; Banks, B. P.; Grooms, G. M.; Sperlich, A.; Dyakonov, V.; Beaupre, S.; Leclerc, M.; Xu, T.; Yu, L. P.; Poluektov, O. G. Highly-Efficient Charge Separation and Polaron Delocalization in Polymer-Fullerene Bulk-Heterojunctions: A Comparative Multi-Frequency EPR and DFT Study. *Phys. Chem. Chem. Phys.* **2013**, *15*, 9562−9574.

(18) Wenger, O. S.; Leigh, B. S.; Villahermosa, R. M.; Gray, H. B.; Winkler, J. R. Electron Tunneling Through Organic Molecules in Frozen Glasses. *Science* **2005**, *307*, 99−102.

(19) Lewis, F. D.; Wu, T.; Zhang, Y.; Letsinger, R. L.; Greenfield, S. R.; Wasielewski, M. R. Distance-Dependent Electron Transfer in DNA Hairpins. *Science* **1997**, *277*, 673−676.

(20) Davis, W. B.; Svec, W. A.; Ratner, M. A.; Wasielewski, M. R. Molecular-Wire Behaviour in *p*-Phenylenevinylene Oligomers. *Nature* **1998**, *396*, 60−63.

(21) Goldsmith, R. H.; Sinks, L. E.; Kelley, R. F.; Betzen, L. J.; Liu, W. H.; Weiss, E. A.; Ratner, M. A.; Wasielewski, M. R. Wire-like Charge Transport at near Constant Bridge Energy through Fluorene Oligomers. *Proc. Natl. Acad. Sci. U. S. A.* **2005**, *102*, 3540−3545.

(22) Poluektov, O. G.; Filippone, S.; Martin, N.; Sperlich, A.; Deibel, C.; Dyakonov, V. Spin Signatures of Photogenerated Radical Anions in Polymer−[70]Fullerene Bulk Heterojunctions: High Frequency Pulsed EPR Spectroscopy. *J. Phys. Chem. B* **2010**, *114*, 14426−14429.

(23) Jiang, X. M.; Österbacka, R.; Korovyanko, O.; An, C. P.; Horovitz, B.; Janssen, R. A. J.; Vardeny, Z. V. Spectroscopic Studies of Photoexcitations in Regioregular and Regiorandom Polythiophene Films. *Adv. Funct. Mater.* **2002**, *12*, 587−597.

(24) Lilliu, S.; Agostinelli, T.; Pires, E.; Hampton, M.; Nelson, J.; Macdonald, J. E. Dynamics of Crystallization and Disorder during Annealing of P3HT/PCBM Bulk Heterojunctions. *Macromolecules* **2011**, *44*, 2725−2734.

(25) Kayunkid, N.; Uttiya, S.; Brinkmann, M. Structural Model of Regioregular Poly(3-hexylthiophene) Obtained by Electron Diffraction Analysis. *Macromolecules* **2010**, *43*, 4961−4967.

(26) Fukuju, T.; Yashiro, H.; Maeda, K.; Murai, H.; Azumi, T. Singlet-Born SCRP Observed in the Photolysis of Tetraphenylhydrazine in an SDS Micelle: Time Dependence of the Population of the Spin States. *J. Phys. Chem. A* **1997**, *101*, 7783−7786.

(27) Grzegorczyk, W. J.; Savenije, T. J.; Dykstra, T. E.; Piris, J.; Schins, J. M.; Siebbeles, L. D. A. Temperature-Independent Charge Carrier Photogeneration in P3HT-PCBM Blends with Different Morphology. *J. Chem. Phys. C* **2010**, *114*, 5182−5186.

(28) Liu, T.; Troisi, A. Absolute Rate of Charge Separation and Recombination in a Molecular Model of the P3HT/PCBM Interface. *J. Phys. Chem. C* **2011**, *115*, 2406−2415.

(29) Till, U.; Klenina, I. B.; Proskuryakov, I. I.; Hoff, A. J.; Hore, P. J. Recombination Dynamics and EPR Spectra of the Primary Radical Pair in Bacterila Photosynthetic Reaction Centers with Blocked Electron Transfer to the Primary Acceptor. *J. Phys. Chem. B* **1997**, *101*, 10939−10948.

(30) Vukmirović, N.; Wang, L. W. Carrier Hopping in Disordered Semiconducting Polymers: How Accurate is the Miller−Abrahams Model? *Appl. Phys. Lett.* **2010**, *97*, 043305.

(31) Yuan, Y.; Zhang, J.; Sun, J.; Hu, J.; Zhang, T.; Duan, Y. Polymorphism and Structural Transition around 54 C° in Regioregular Poly(3-hexylthiophene) with High Crystallinity As Revealed by Infrared Spectroscopy. *Macromolecules* **2011**, *44*, 9341−9350.

(32) Kobori, Y.; Sekiguchi, S.; Akiyama, K.; Tero-Kubota, S. Chemically Induced Dynamic Electron Polarization Study on the Mechanism of Exchange Interaction in Radical Ion Pairs Generated by Photoinduced Electron Transfer Reactions. *J. Phys. Chem. A* **1999**, *103*, 5416−5424.

(33) Scott, A. M.; Miura, T.; Ricks, A. B.; Dance, Z. E. X.; Giacobbe, E. M.; Colvin, M. T.; Wasielewski, M. R. Spin-Selective Charge Transport Pathways through *p*-Oligophenylene-Linked Donor-Bridge-Acceptor Molecules. *J. Am. Chem. Soc.* **2009**, *131*, 17655−17666.
(34) Marcus, R. A.; Sutin, N. Electron Transfer in Chemistry and Biology. *Biochim. Biophys. Acta* **1985**, *811*, 265−322.
(35) Miller, J. R.; Beitz, J. V. Long-Range Transfer of Positive Charge between Dopant Molecules in a Rigid Glassy Matrix. *J. Chem. Phys.* **1981**, *74*, 6746−6756.
(36) Lewis, F. D.; Letsinger, R. L.; Wasielewski, M. R. Dynamics of Photoinduced Charge Transfer and Hole Transport in Synthetic DNA Hairpins. *Acc. Chem. Res.* **2001**, *34*, 159−170.
(37) McConnell, H. Intramolecular Charge Transfer in Aromatic Free Radicals. *J. Chem. Phys.* **1961**, *35*, 508−515.
(38) Kobori, Y.; Yago, T.; Akiyama, K.; Tero-Kubota, S.; Sato, H.; Hirata, F.; Norris, J. R. Superexchange Electron Tunneling Mediated by Solvent Molecules: Pulsed Electron Paramagnetic Resonance Study on Electronic Coupling in Solvent-Separated Radical Ion Pairs. *J. Phys. Chem. B* **2004**, *108*, 10226−10240.
(39) Voityuk, A. A.; Rosch, N.; Bixon, M.; Jortner, J. Electronic Coupling for Charge Transfer and Transport in DNA. *J. Phys. Chem. B* **2000**, *104*, 9740−9745.
(40) Lan, Y.-K.; Huang, C.-I. A Theoretical Study of the Charge Transfer Behavior of the Highly Regioregular Poly-3-hexylthiophene in the Ordered State. *J. Phys. Chem. B* **2008**, *112*, 14857−14862.